



Cite this: *Chem. Sci.*, 2025, **16**, 5640

All publication charges for this article have been paid for by the Royal Society of Chemistry

Received 17th January 2025

Accepted 13th February 2025

DOI: 10.1039/d5sc00438a

[rsc.li/chemical-science](http://rsc.li/chemical-science)

## Introduction

Ether linkages are ubiquitous in a myriad of natural products, pharmaceuticals, and agrochemicals (Scheme 1a).<sup>1</sup> In particular, branched allyl aryl ethers linkages constitute a significant molecular framework that functions as versatile building blocks for a wide range of organic transformations, and various methods have been developed toward their synthesis.<sup>2</sup> Among them, the palladium-catalyzed Tsuji–Trost reaction represents one of the most powerful and robust methods to prepare these motifs by using allylic electrophiles with oxygen nucleophiles (Scheme 1b, left).<sup>3</sup> However, accessing pre-functionalized alkenes bearing a leaving group at the allylic position often requires extra synthetic effort. In addition, substituted alkenes, especially internal alkenes, often yield products with unsatisfactory regio- and diastereoselectivity, ultimately limiting the scope of this approach. The direct transition-metal-catalyzed alkene hydroetherification provides a complementary and economical approach using simple and easily available starting materials.<sup>4</sup> In this regard, various oxygen nucleophiles, including carboxylic acids, alcohols, and ketoximes, have been extensively utilized over the years toward coupling with a variety

of alkenes.<sup>5</sup> However, much less progress has been made with respect to the reactions using simple phenols with 1,3-dienes in catalytic hydroetherification (Scheme 1b, right). This is largely due to the inherent electron-rich structure of phenols, which leads to competitive chemoselectivity between forming the C–O bond (O-allylation)<sup>6</sup> and the C–C bond (C-allylation) with *ortho* or *para* C–H bonds.<sup>7</sup> Additionally, conjugated dienes are typically converted into the corresponding 1,2- and/or 1,4-addition products through metal–π-allyl intermediates. Notably, although significant advancements have been made recently in the highly chemo- and regioselective hydrofunctionalization of 1,3-dienes with phenols for C-allylation,<sup>8</sup> there is a notable scarcity in the selective O-allylation of phenols with conjugated dienes to facilitate the intriguing hydroetherification process, which greatly arouses our interest.

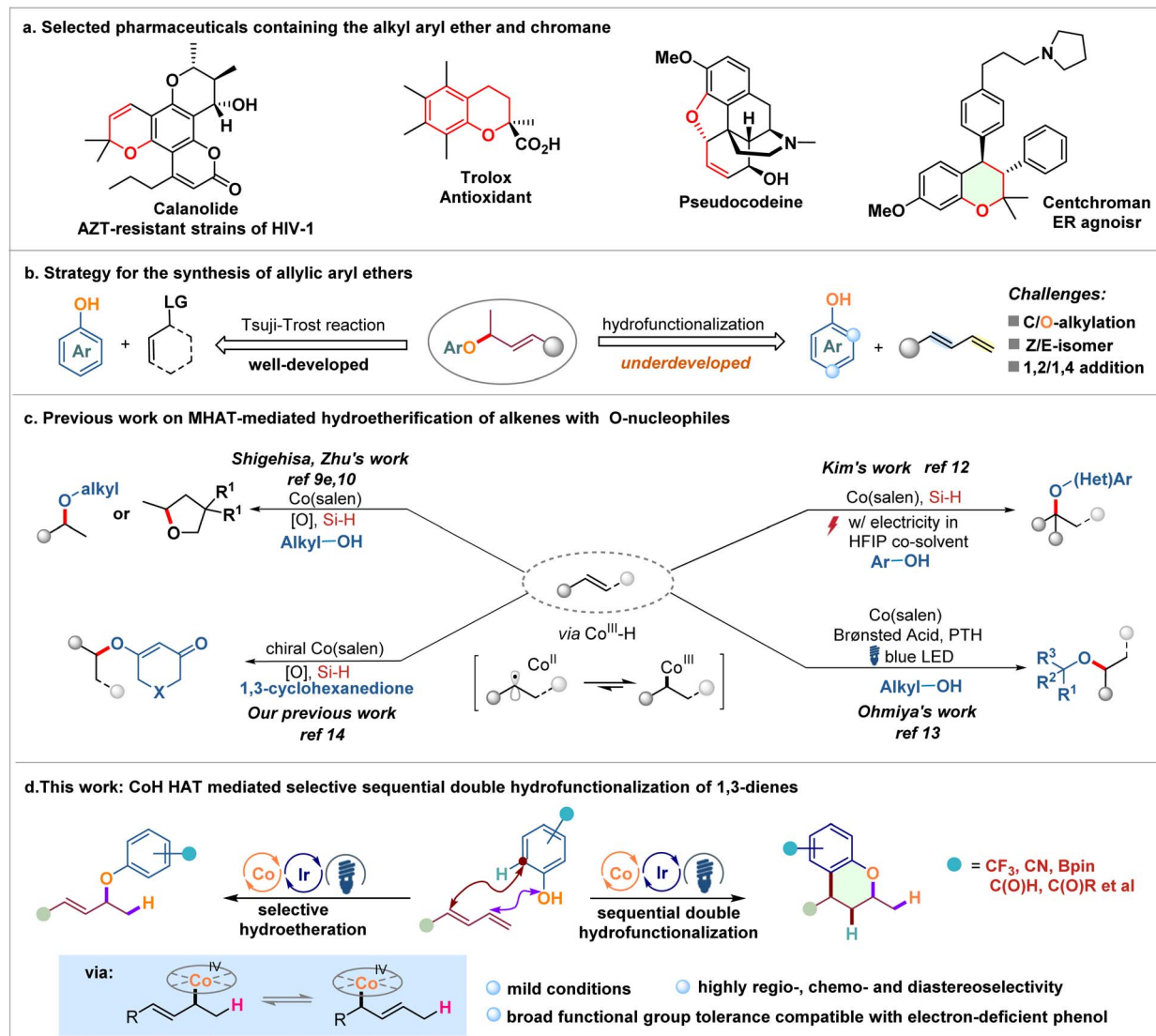
Recently, the emerging cobalt(salen)-catalyzed hydrogen atom transfer (HAT) reactions of alkenes with nucleophiles involving a high-valent alkylcobalt(IV) intermediate have emerged as a versatile platform for alkene hydrofunctionalization (Scheme 1c).<sup>9</sup> Specifically, by employing Co(salen) catalyst combinations with hydrosilanes and peroxide or *N*-fluoro species, an array of cobalt-catalyzed intra- and intermolecular hydroalkoxylation reactions of alkenes with alcohol nucleophiles have been achieved.<sup>9e,10</sup> This efficient oxidative metal–hydride HAT catalytic system was further developed by Zhu to allow for electrocatalytic oxidative hydroalkoxylation, eliminating the need for stoichiometric chemical oxidants.<sup>11</sup> In 2022, Kim reported an electrocatalytic hydroetherification of alkenes with phenols, facilitating the modular synthesis of alkyl aryl ethers in high yields.<sup>12</sup> Meanwhile, Ohmiya demonstrated a novel photoredox/cobalt-catalyzed

<sup>a</sup>Jilin Province Key Laboratory of Organic Functional Molecular Design & Synthesis, Department of Chemistry, North-East Normal University, Changchun 130024, China. E-mail: [zhangg492@nenu.edu.cn](mailto:zhangg492@nenu.edu.cn)

<sup>b</sup>State Key Laboratory of Organometallic Chemistry, Shanghai Institute of Organic Chemistry, Chinese Academy of Sciences, Shanghai 200032, China

† Electronic supplementary information (ESI) available. CCDC 2351059. For ESI and crystallographic data in CIF or other electronic format see DOI: <https://doi.org/10.1039/d5sc00438a>





**Scheme 1** Representative ether-containing compounds and methods for constructing branched allyl aryl ether linkages, as well as the hydrofunctionalization of alkenes with phenols.

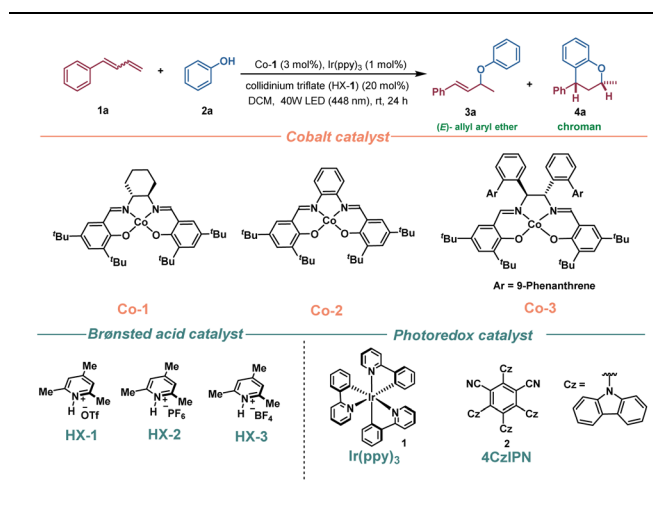
hydroetherification of alkenes using catalytic amounts of weak Brønsted acid instead of stoichiometric silanes as a hydrogen supply to generate the putative  $\text{Co}(\text{III})\text{-H}$  species.<sup>13</sup> These methods provide a convenient and promising synthetic approach for C–O bond construction *via* a radical-polar cross-over process. More recently, our research group successfully achieved enantioselective hydroetherification of alkenes by utilizing a chiral Co(salen) catalyst, which performed through a CoH-mediated oxidative metal-hydride hydrogen atom transfer (MHAT) process using symmetric 1,3-diketones as oxygen nucleophiles, thus enabling the synthesis of chiral alkyl ethers.<sup>14</sup> Despite these accomplishments, the expansion of this intriguing approach to investigate allyl cobalt(IV) complexes<sup>15</sup> for selective and divergent hydrofunctionalization of 1,3-dienes with nucleophiles has not yet been established. Our continued interest in Co-catalyzed MHAT reactions<sup>14,16</sup> has led us to report a photoredox/cobalt-catalyzed radical-polar crossover

hydroetherification of dienes with phenol feedstocks (Scheme 1d). Interestingly, a selective sequential hydroetherification/hydroarylation process can also be achieved by prolonging the reaction time, yielding a variety of value-added chroman derivatives<sup>17</sup> in good to excellent yields and stereoselectivity. This divergent transformation represents the first example of MHAT-mediated selective sequential double hydrofunctionalization to forge radical-involved C–O and C–C bonds in a single operation.

## Results and discussion

We initiated our investigation by subjecting 1-phenyl-1,3-butadiene (**1a**) and phenol (**2a**) as model substrates to optimize the hydroetherification reaction conditions under photo- and cobalt dual catalysis (Table 1). The standard conditions included the use of a 1,2-cyclohexadiamine-derived Co(salen)



Table 1 Optimization of the reaction conditions<sup>a</sup>

<sup>a</sup> Reaction conditions: the reaction was carried out with **1a** (0.4 mmol), **2a** (0.2 mmol), photoredox catalyst (0.002 mmol), Co catalyst (0.006 mmol), and Brønsted acid catalyst (0.04 mmol) in DCM (1.0 mL) under 40 W blue LED (448 nm) irradiation for 24 h. <sup>b</sup> Yield was determined by <sup>1</sup>H NMR spectroscopy using CH<sub>2</sub>Br<sub>2</sub> as an internal standard. <sup>c</sup> The values of dr were determined by <sup>1</sup>H NMR spectroscopy.

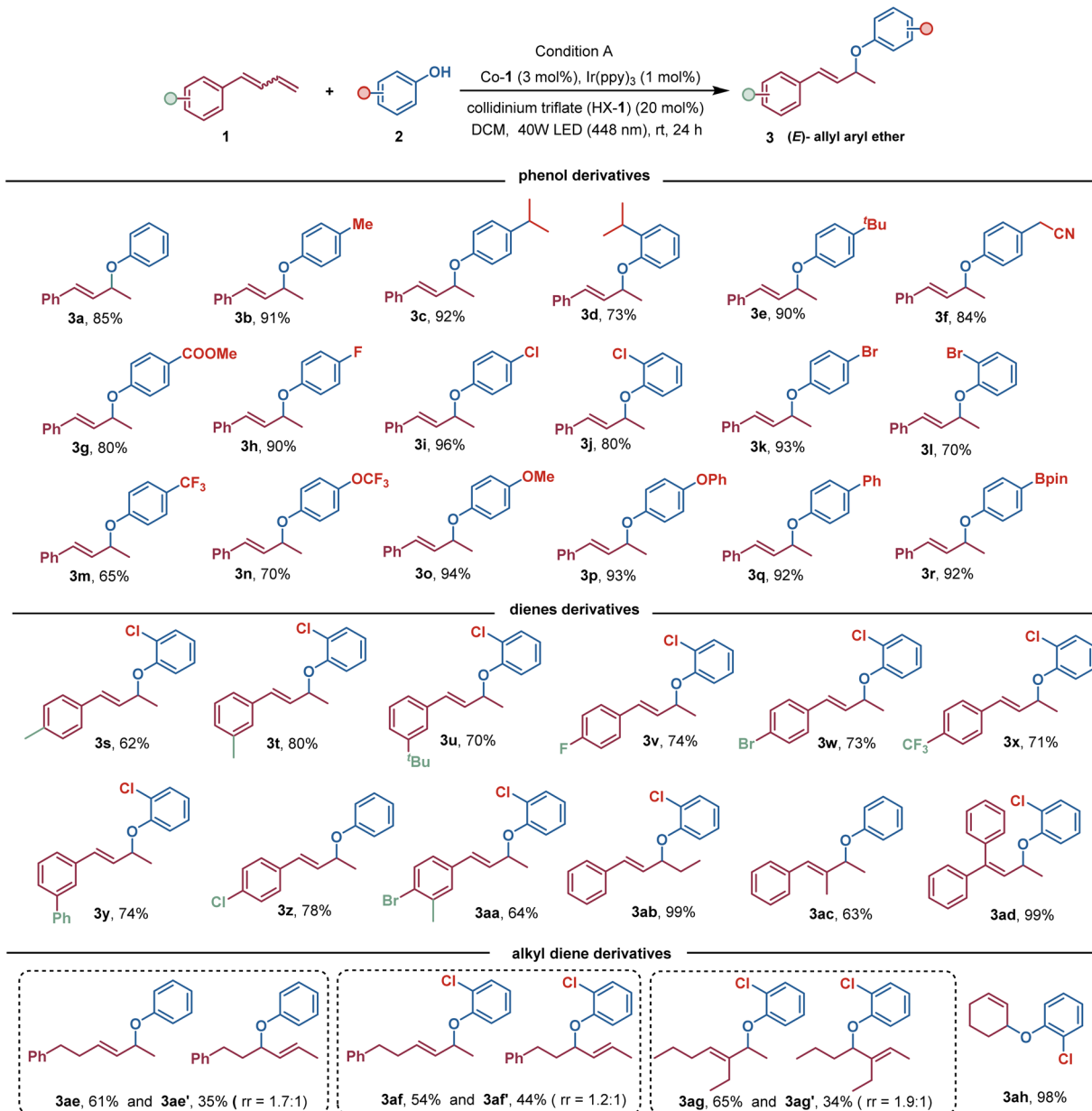
complex (**Co-1**) as the catalyst, Ir(ppy)<sub>3</sub> as the photocatalyst, and collidinium triflate (HX-1) as a proton shuttle in DCM at room temperature under 40 W blue LED irradiation, which delivered (*E*)-allylic ether **3a** in 85% yield with excellent regioselectivity (>20 : 1 rr) (Table 1, entry 1). Based on previous reports, Ir(ppy)<sub>3</sub> exhibits a high excited-state reduction potential of  $E_{1/2}$  [Ir<sup>III\*</sup>]/[Ir<sup>IV</sup>] = -1.73 V vs. SCE, and its reductively quenched congener possesses a moderate oxidation potential of  $E_{1/2}$  [Ir<sup>IV</sup>]/[Ir<sup>III</sup>] = 0.77 V vs. SCE.<sup>18</sup> This enables the single-electron reduction of Co(II) [ $E_{\text{red}}$  (**Co-1**) = -1.60 V vs. SCE] and the single-electron oxidation of alkyl-Co(III) [ $E_{\text{ox}}$  (**Co-1**) = 0.00 V vs. Fc<sup>+</sup>/Fc],<sup>19</sup> thereby facilitating the hydroetherification reaction of 1,3-dienes under redox-neutral catalytic conditions. Control experiments demonstrated that light, photocatalyst, the cobalt salen catalyst, and the collidinium ion were all necessary for the reaction (Table 1, entries 2 and 3).

The use of cobalt catalyst, **Co-2**, delivered a 78% yield of product **3a**, whereas the utilization of **Co-3**, resulted in a significant reduction in yield (entries 4 and 5). Using triflic

acid, instead of HX-1, failed to deliver the expected product **3a** (entry 6). Substituting 2,4,6-collidine for HX-1 resulted in the failure to produce the expected allylic aryl ether **3a**, suggesting that the collidinium ion is responsible for Co(II) protonation.<sup>20</sup> Other collidinium salts, such as HX-1 and HX-2, failed to produce the expected hydroetherification product **3a**, likely due to insufficient acidity for protonation of the cobalt(II) species to generate the key CoH necessary for the MHAT process (entries 8 and 9). Additionally, when employing an organic photocatalyst, such as 4CzIPN, no production of **3a** was observed (entry 10). Switching the solvent from DCM to MeCN resulted in a significant decrease in yield (entry 11). Furthermore, the observation that using (*E*)-**1a**, (*Z*)-**1a**, or a mixture of 1,3-diene **1a** (*E/Z* = 1 : 1.5) consistently yielded (*E*)-**3a** indicates that the configuration of the dienes has little effect on reaction efficiency (see ESI Table S3†). Notably, prolonging the reaction time to 48 h led to the observation of sequential double hydrofunctionalization of 1,3-dienes with phenol, resulting in the formation of chroman **4a** (83% yield, 3.3 : 1 dr), which are important pharmacophores in medicinal chemistry and biomedical fields (Table 1, entry 12). To our delight, excellent diastereoselectivity (>20 : 1) was observed when substituting 2-chlorophenol for phenol, which delivered the expected chroman derivative **4b** in 85% yield (entry 13).

With these optimized reaction conditions in hand, we then examined the substrate scope of this photoredox/cobalt-catalyzed hydrofunctionalization. As illustrated in Scheme 2, we first investigated the generality of this method for selective hydroetherification of 1,3-dienes. It was found that an array of phenols bearing a variety of functional groups, including -alkyl, -aryl, -OCH<sub>3</sub>, -CN, -COOMe, -F, -Cl, -Br, -OCF<sub>3</sub>, and -CF<sub>3</sub>, could be effectively alkylated with 1,3-diene **1a** to deliver the corresponding (*E*)-allylic aryl ether products in generally good to excellent yields with exclusive regio- and stereoselectivities. The accommodation of boronic acid pinacol ester (**3r**) and aryl halides (**3i**-**3l**) provided more opportunities for further elaborations. In addition, a wide range of 1,3-dienes bearing either electron-donating functional groups or electron-withdrawing functional groups on the aromatic rings were well tolerated under this reaction condition, providing the expected products **3s**-**3aa** in good to excellent yields. Additionally, internal alkenes, as demonstrated for penta-1,3-dien-1-ylbenzene, were also valid substrates for this selective hydroetherification, furnishing the corresponding product **3ab** in quantitative yield. Interestingly, conjugated dienes with steric hindrance were also viable to deliver the expected regioselective hydroetherification products **3ac** and **3ad** in 62% and 99% yield, respectively. These exciting results stimulated us to evaluate whether a wider scope of 1,3-dienes, such as alkyl-substituted alkenes, were amenable to this CoH-mediated hydroetherification. Delightedly, an assortment of alkyl-substituted 1,3-dienes can be efficiently transformed into the desired (*E*)-allyl aryl ether products, **3ae**-**3ag**, in generally favourable yields with simultaneous formation of the competitive 1,4-hydroetherification product. 1,3-Cyclobutadiene can be reacted to produce a sole hydroetherification product **3ah** in 98% yield.

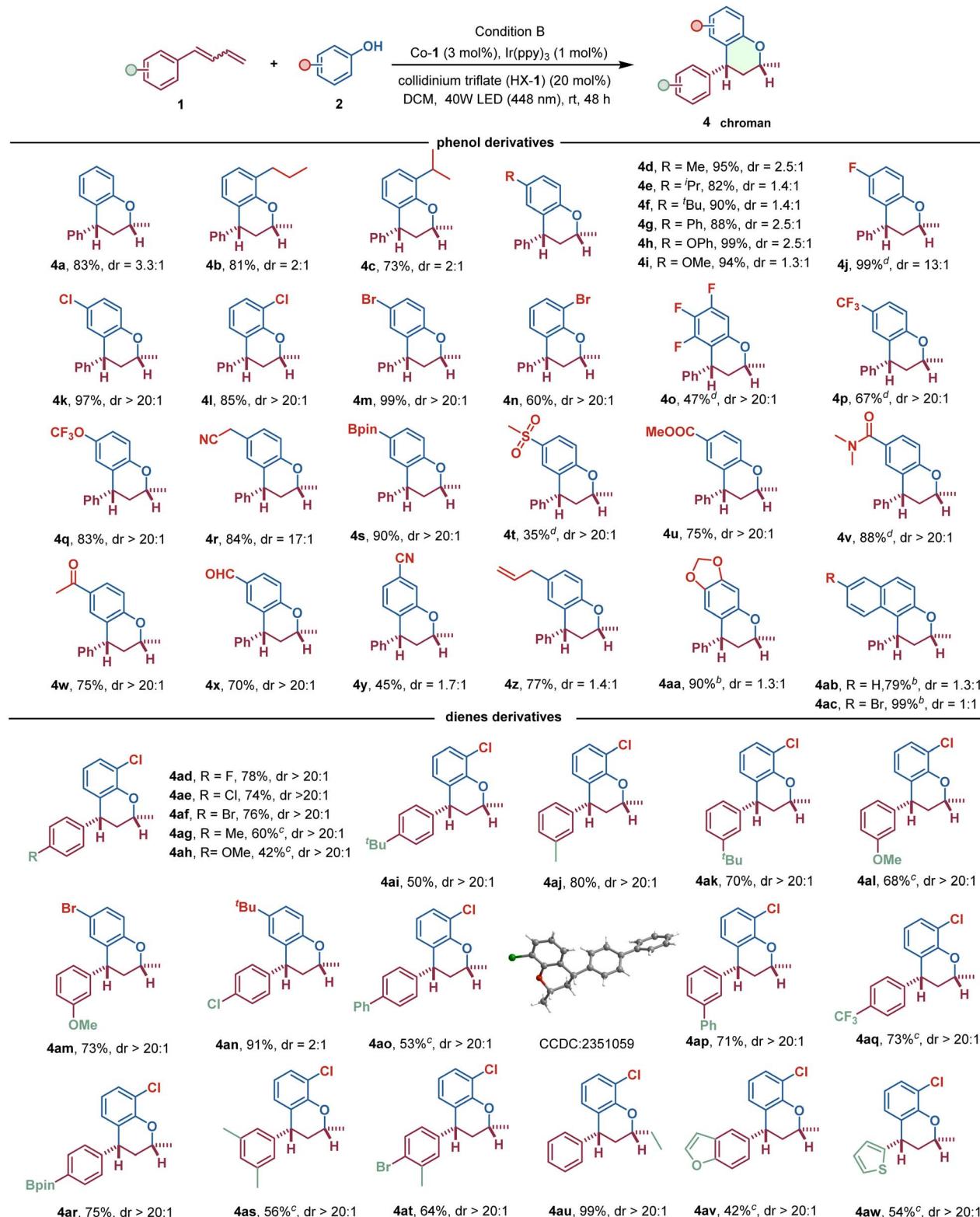




**Scheme 2** Substrate scope of hydroetherification reaction of 1,3-dienes with phenols.<sup>a</sup> Reaction condition: phenols (0.2 mmol), 1,3-dienes (2.0 equiv.), HX-1 (20 mol%), Ir(ppy)<sub>3</sub> (1 mol%), and [Co]-1 (3 mol%) in dry dichloromethane (1.0 mL) under 40 W blue LED (448 nm) at room temperature for 24 h. Isolated yields.

Next, we investigated the potential sequence of double hydrofunctionalization reaction of 1,3-dienes with phenols to construct chroman derivatives in a single operation (Scheme 3). To our delight, this catalytic system could be successfully extended to a broad range of 1,3-dienes and phenols, showcasing generally high catalytic efficiency, providing chroman derivatives in good to excellent yields and stereoselectivity. A brief exploration of the phenol substrates revealed that the presence of an electron-withdrawing substituent on the aromatic ring in phenols was beneficial to improve the diastereoselective control in double hydrofunctionalization reaction compared to phenols with electron-donating functional groups (**4b–4i** vs. **4j–4x**). Hence, several phenols bearing

electron-withdrawing substituents, including –F, –Cl, –Br, –CF<sub>3</sub>, –OCF<sub>3</sub>, –CN, –CHO, COMe, –COOMe, –CON(Me)<sub>2</sub>, –SO<sub>2</sub>Me, and –Bpin, reacted with **1a** to give the corresponding chroman derivatives in good to excellent yields with up to 20 : 1 diastereoselective control. The high compatibility of this reaction with electron-withdrawing groups significantly enhances the molecular complexity and provides a valuable complement to chroman derivatives that were inaccessible through previous strategies.<sup>17</sup> Due to the high reactivity of the phenols with electron-donating functional groups (such as alkyl and alkoxy), the diastereoselective control of the sequential hydroetherification/hydroarylation reaction is relatively poor, and the resulting chroman products have a high yield but with

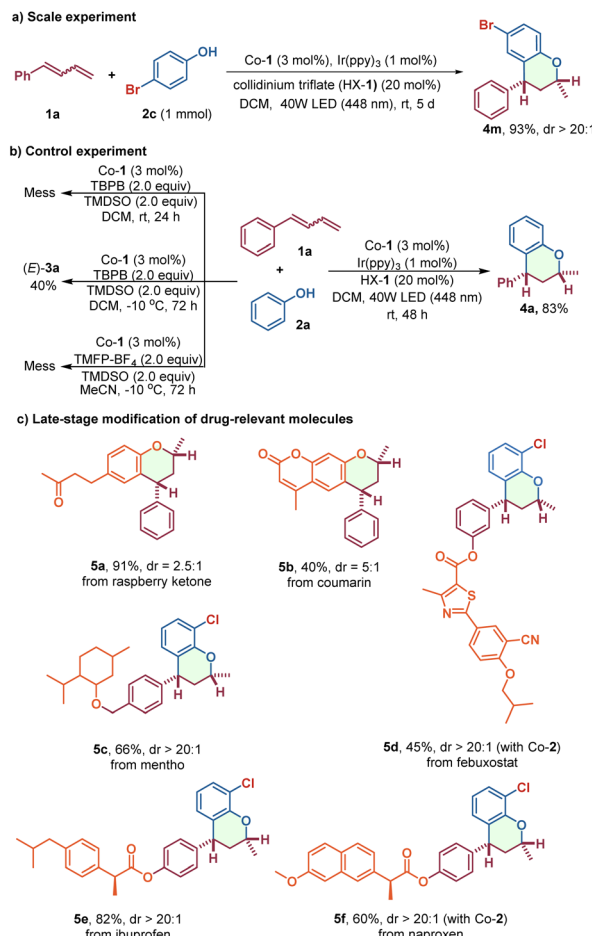


**Scheme 3** The substrate scope of dihydrofunctionalization reaction of 1,3-dienes with phenols. <sup>a</sup>Reaction condition: phenols (0.2 mmol), 1,3-dienes (2.0 equiv.), HX-1 (20 mol%), Ir(ppy)<sub>3</sub> (1 mol%), and [Co]-1 (3 mol%) in dry dichloromethane (1.0 mL) under 40 W blue LED (448 nm) at room temperature for 48 h. <sup>b</sup>Reaction conditions: 1,3-dienes (0.2 mmol), phenols (2.0 equiv.), HX-1 (20 mol%), Ir(ppy)<sub>3</sub> (1 mol%), and [Co]-1 (3 mol%) in dry dichloromethane (1.0 mL) under 40 W blue LED (448 nm) at room temperature for 24 h. <sup>c</sup>4 Å (10 mg) was added. <sup>d</sup>Prolonging the reaction time to 72 h.

approximately 2 : 1 diastereomeric ratio. In addition, the steric hindrance of substituents in phenols also influences the efficiency of the sequential double hydrofunctionalization of **1a**. For instance, the yield of the reaction using *para*-isopropyl-substituted phenol is notably superior to that of *o*-isopropyl-substituted phenol (**4c** vs. **4e**), which is also demonstrated with the reaction using *p*-Br- and *o*-Br-substituted phenols (**4m** vs. **4n**). We hypothesize that the discrepancy may be due to steric hindrance caused by the bulky spatial volume at the *ortho*-site of the phenols, which hinders the nucleophilic substitution process of the alkylcobalt(IV) intermediates. The generality of this reaction was further highlighted by the incorporation of aldehyde, allyl, and cyano groups to afford the corresponding products, **4x**–**4z**. The good functional-group tolerance, particularly those susceptible to CoH catalytic systems, offers a lot of opportunities for further chemical transformations. In addition to these simple phenols, electron-rich aromatics, such as sesamol and 2-naphthol, were also viable substrates, all of which can undergo this sequential hydroetherification/hydroarylation reaction to deliver chroman derivatives **4aa**–**4ac** in up to 99% yield, albeit with relatively low diastereoccontrol. Interestingly, the diastereoccontrol for this selective sequential double hydrofunctionalization process mediated by CoH HAT appears to be less reliant on the electronic and spatial effects of the diene substrates. A broad spectrum of 1,3-dienes with either electron-withdrawing functional groups or electron-donating groups were all viable coupling partners, delivering a variety of chroman derivatives in good to excellent yields with >20 : 1 dr. The position of the substituent on the phenyl ring in 1,3-dienes almost did not alter the diastereoselectivity, as demonstrated with the methyl (**4ag**, **4aj**), tertiary butyl (**4ai**, **4ak**), phenyl (**4ao**, **4ap**), and methoxy (**4al**, **4am**), albeit with discrepancy in product yields. The configuration of the product **4ao** was unequivocally determined by single-crystal X-ray diffraction. Additionally, internal alkene could undergo this transformation to afford corresponding chroman **4au** in 99% yield and >20 : 1 dr. Heteroaryl-substituted 1,3-dienes were also competent to furnish the products, **4av** and **4aw**, in moderate yields. However, the alkyl-substituted 1,3-dienes only provided excellent yield of allylic aryl ethers under these reaction conditions, with no sequential double hydrofunctionalization products observed. This may be attributed to the decreased reactivity of the unactivated internal olefin generated after the first hydroetheration, as well as the presumed instability of the alkyl-cobalt intermediates during the second hydrofunctionalization.

Overall, this protocol exhibits excellent tolerance towards a wide range of strong electron-withdrawing substituents, whether in olefin or phenol nucleophiles, representing a significant advancement over traditional Friedel–Crafts strategies for synthesizing chroman derivatives.

With the aim of further extending the synthetic utility of this methodology, a 1 mmol-scale synthesis was conducted to demonstrate the practicability of this method, and the target chroman **4m** was obtained in good yield (Scheme 4a). In addition, a comparison with conventional MHAT reactions using superstoichiometric chemical oxidants highlights the unique advantages of this photoredox/cobalt catalytic system

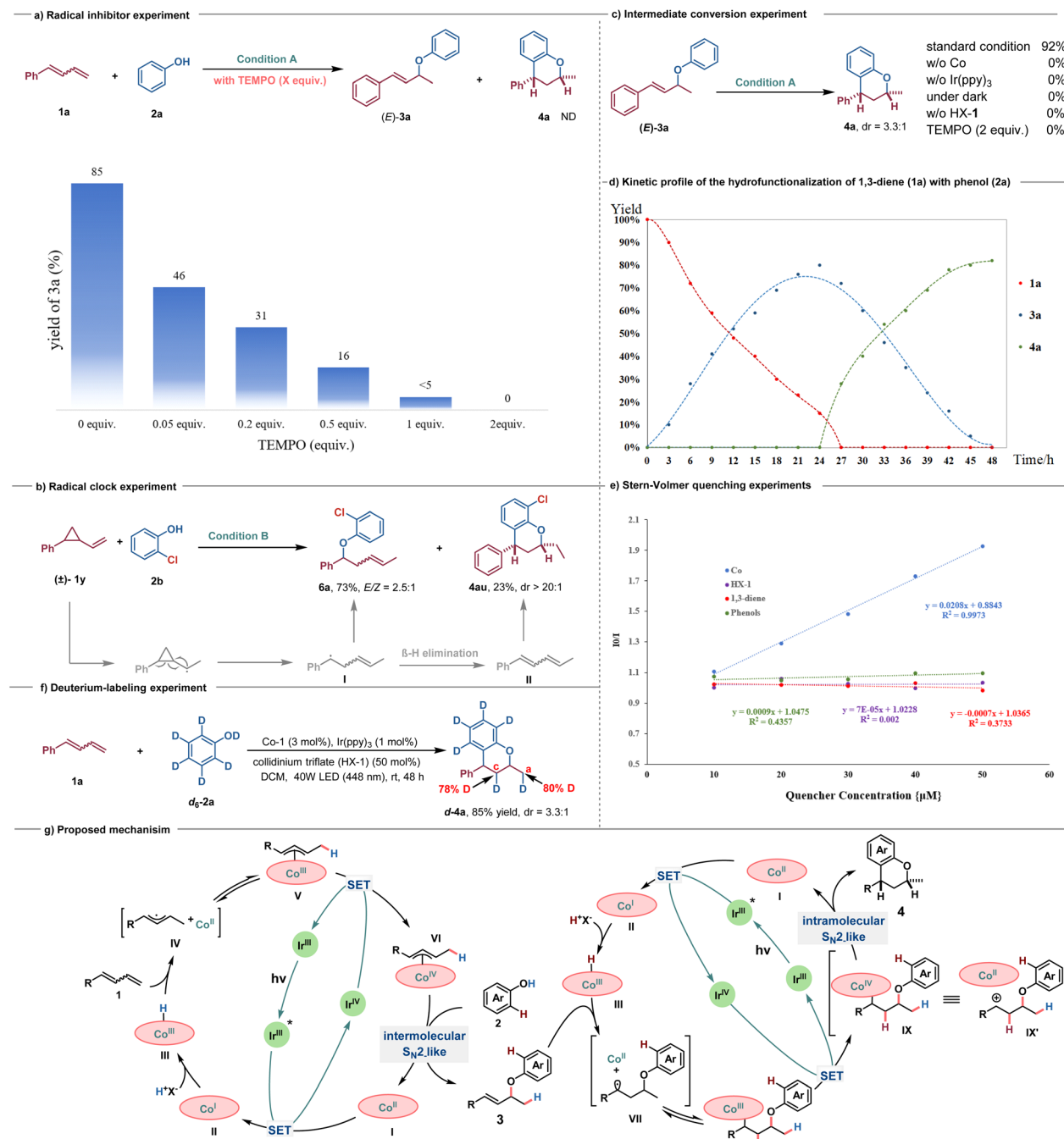


Scheme 4 Synthetic applications.

(Scheme 4b). To illustrate, some bioactive molecules, such as raspberry ketone, coumarin, and structurally more complicated menthol, febuxostat, ibuprofen, and naproxen-derived alkenes were conveniently transformed to the corresponding chroman derivatives, **5a**–**5f**, in one step, which demonstrated that this method would be suitable for late-stage functionalization of complex bioactive compounds (Scheme 4c).

To gain some insights into the mechanism of this transformation, several control experiments were performed. As expected, upon the addition of radical inhibitors, such as 2,2,6,6-tetramethyl-1-piperidinyloxy (TEMPO), into the model reaction, the formation of **3a** was inhibited (Scheme 5a). In addition, the radical-clock experiment using (2-vinylcyclopropyl)-benzene **1v** resulted in the formation of ring-opening/C–O formation product **6a** in 73% yield with *E/Z* = 2.5 : 1, which may be attributed to the  $\beta$ -hydrogen elimination of alkyl radical intermediate **I**, leading to the production of 1,3-diene **II**, followed by a sequential double hydrofunctionalization process resulting in the delivery of **4au** (Scheme 5b). These phenomena suggest that a radical intermediate is possibly involved in this transformation, in line with the speculated CoH-mediated HAT process. We also conducted the reaction using isolated **3a** as the substrate under standard conditions, resulting in the identical product **4a** with a yield of 92% (Scheme 5c). Considering the





**Scheme 5** Mechanistic investigation and proposed mechanism (a) radical inhibition experiment. (b) Radical-clock experiment. (c) Intermediate conversion experiment. (d) Kinetic profile of the hydrofunctionalization of 1,3-diene (**1a**) with phenol (**2a**). (e) Stern–Volmer quenching experiments. (f) Deuterium-labeling experiment. (g) Proposed mechanism.

possibility of Lewis acid or Brønsted acid promoting intramolecular Friedel–Crafts acylation of **3a** to form **4a**,<sup>21</sup> a series of control experiments were performed. The results showed that light, cobalt catalyst, photosensitizer, and Brønsted acid are all essential for the formation of **4a** (Scheme 5c). To gain further insights into the dynamic progress of the reaction, we monitored the amounts of **1a**, **3a**, and **4a** over time (Scheme 5d). Within the initial 24 h, there was a gradual accumulation of

product **3a**, with almost undetectable levels of **4a**. The highest yield of **3a** was achieved at 24 h. Subsequently, there was a rapid consumption of **3a** over the following 24 h, gradually converting it to **4a** until completion. The Stern–Volmer quenching experiments further indicated that photoexcited Ir(III)\* could be quenched by the Co catalyst rather than by HX-1, 1,3-dienes, or phenols (Scheme 5e). Additionally, a deuterium-labeled experimental reaction of **1a** using phenol-**d**<sub>6</sub> (**d**<sub>6</sub>-**2a**) as the



nucleophile was conducted, yielding **d-4a** in 85% yield with a 3.3:1 dr, and 80% and 78% deuterium incorporation into carbons C(a) and C(c) of the product, respectively (Scheme 5f). These results demonstrated that proton transfer occurred from the O–D group of **d**-phenol to the 1,3-dienes in both hydrofunctionalization processes. The deuterium incorporation of no more than 80% suggested that HX-1 serves as the proton shuttle in the Co(III)H-mediated MHAT process, with part of the hydrogen source coming from HX-1 itself.

Based on these experimental results and literature precedents, a possible catalytic cycle for this photoredox/cobalt-catalyzed selective mono- and dihydrofunctionalization is shown in Scheme 5g. Under visible light irradiation, the Ir(III) catalyst transitions to the excited state Ir(III)\*, bearing high reducing ability, which undergoes a single electron transfer (SET) to SalenCo(II) to form SalenCo(I) and Ir(IV) species.<sup>9d,13</sup> The low-valent Co(I) then reacts with a proton in collidinium triflate (HX-1) to form the putative Co(III)–H species **III**.<sup>22,23</sup> Subsequently, a Co(III)–H mediated MHAT to alkenes could yield a metallic cobalt(II) and an allylic radical pair **IV**, which are in fast equilibrium with allylcobalt(III) species **V**.<sup>9a,24–28</sup> A further SET oxidation of allylcobalt(III) species **V** by Ir(IV) generates the pivotal allylcobalt(IV) species **VI**, which undergoes an intermolecular S<sub>N</sub>2-substitution reaction with the phenol nucleophile to afford the expected allyl aryl ether **3** and regenerate Co(II), thus closing the catalytic cycle.<sup>15,29–34</sup> Thereafter, allyl aryl ether **3** could undergo a similar cobalt(III)H-mediated MHAT process by participating in an intramolecular nucleophilic substitution reaction involving benzylcobalt(IV) species **IX** with phenol as the carbon-based nucleophile for C–C bond construction to deliver chromans **4**. Given that Co-MHAT catalysis for alkene substrates involving cation-stabilizing groups (such as benzylic or tertiary carbocations) has proposed a carbocation–Co(II) ion pair alongside Co(IV)–alkyl species,<sup>19,35</sup> the possibility of direct cyclization *via* carbocation **IX'** during the second nucleophilic cyclization cannot be excluded.

## Conclusions

By exploiting a photoredox catalysis combined with Co catalysis, we have accomplished the first highly selective, divergent mono- and dihydrofunctionalization of simple 1,3-dienes with phenols, thereby enabling an efficient and alternative strategy to access allylic aryl ethers and valuable chroman derivatives *via* Co(III)H-mediated MHAT, followed by S<sub>N</sub>2-substitution of key alkyl–Co(IV) with nucleophiles. This radical-based strategy features high atom economy; broad functional group tolerance; high regio-, chemo-, and diastereoselectivity; and enables the installation of electron-poor groups that are typically not compatible with previous Friedel–Crafts reactions. Meanwhile, this reaction can be used in the last-stage functionalization of complex bioactive compounds. The continuous and selective formation of C–O and C–C bonds expands the application range of cobalt–hydride MHAT reaction and offers new opportunities for the future design and synthesis of heterocyclic molecules. Further investigations on the enantioselective version and the development of new cobalt catalytic systems and their

application in selective, divergent MHAT hydrofunctionalization are underway in our laboratory.

## Data availability

All data supporting the findings of this study including the experimental procedures and characterization of the compounds are available within the article and its ESI.† Crystallographic data for compound **4ao** has been deposited at the CCDC under [CCDC 2351059] and can be obtained free of charge from the Cambridge Crystallographic Data Centre *via* [https://www.ccdc.cam.ac.uk/data\\_request/cif](https://www.ccdc.cam.ac.uk/data_request/cif).

## Author contributions

G. Z. and Q. Z. directed the project. G. Z. conceived the idea, designed the experiments, and wrote the manuscript draft. Y. W. performed the experiments, analyzed the data, and prepared the ESI.† J. M. performed part of the hydroetherification reaction. H. D., D. Z., B. C., and M. G. helped synthesize some substrates and repeated the reactions. All authors participated in the discussion and preparation of the manuscript.

## Conflicts of interest

There are no conflicts to declare.

## Acknowledgements

We thank the NSFC (Grants 22193012, 22171043), and the Fundamental Research Funds for the Central Universities-Excellent Youth Team Program (2412023YQ001).

## Notes and references

- (a) G. Evano, J. Wang and A. Nitelet, Metal-mediated C–O bond forming reactions in natural product synthesis, *Org. Chem. Front.*, 2017, **4**, 2480–2499; (b) W. Schutyser, T. Renders, S. V. Bosch, S.-F. Koelewijn, G. T. Beckham and B. F. Sels, Chemicals from lignin: an interplay of lignocellulose fractionation, depolymerisation, and upgrading, *Chem. Soc. Rev.*, 2018, **47**, 852–908.
- (a) B. M. Trost and F. D. Toste, Enantioselective Total Synthesis of (–)-Galanthamine, *J. Am. Chem. Soc.*, 2000, **122**, 11262–11263; (b) A. M. Kaster, L. Zhu, W. Lyon, R. S. Ammann and A. C. White, Palladium-catalyzed cross-coupling of alcohols with olefins by positional tuning of a counteranion, *Science*, 2024, **385**, 1067–1076; (c) K. Yamada, K. P. S. Cheung and V. Gevorgyan, General Regio- and Diastereoselective Allylic C–H Oxygenation of Internal Alkenes, *J. Am. Chem. Soc.*, 2024, **146**, 18218–18223; (d) Z. Chen, Y. Jiang, L. Zhang, Y. Guo and D. Ma, Oxalic Diamides and tert-Butoxide: Two Types of Ligands Enabling Practical Access to Alkyl Aryl Ethers *via* Cu-Catalyzed Coupling Reaction, *J. Am. Chem. Soc.*, 2019, **141**, 3541–3549; (e) P. M. MacQueen, J. P. Tassone, C. Diaz and



M. Stradiotto, Exploiting Ancillary Ligation To Enable Nickel-Catalyzed C–O Cross-Couplings of Aryl Electrophiles with Aliphatic Alcohols, *J. Am. Chem.*, 2018, **140**, 5023–5027.

3 (a) O. Pàmies, J. Margalef, S. Cañellas, J. James, E. Judge, P. J. Guiry, C. Moberg, J.-E. Bäckvall, A. Pfaltz, M. A. Pericàs and M. Diéguez, Recent Advances in Enantioselective Pd-Catalyzed Allylic Substitution: From Design to Applications, *Chem. Rev.*, 2021, **121**, 4373–4505; (b) C. Li and B. Breit, Rhodium-Catalyzed Dynamic Kinetic Asymmetric Allylation of Phenols and 2-Hydroxypyridines, *Chem. - Eur. J.*, 2016, **22**, 14655–14663.

4 L. Hintermann in *Topics in Organometallic Chemistry*, ed. A. Vigalok, Springer, Berlin, Heidelberg, vol 31, 2010, pp. 123–155.

5 (a) P. T. Marcyk and S. P. Cook, Iron-Catalyzed Hydroamination and Hydroetherification of Unactivated Alkenes, *Org. Lett.*, 2019, **21**, 1547–1550; (b) E. Tsui, A. J. Metrano, Y. Tsuchiya and R. R. Knowles, Catalytic Hydroetherification of Unactivated Alkenes Enabled by Proton-Coupled Electron Transfer, *Angew. Chem., Int. Ed.*, 2020, **59**, 11845–11849; (c) H.-L. Sun, F. Yang, W.-T. Ye, J.-J. Wang and R. Zhu, Dual Cobalt and Photoredox Catalysis Enabled Intermolecular Oxidative Hydrofunctionalization, *ACS Catal.*, 2020, **10**, 4983–4989; (d) T. Song, Y. Luo, K. Wang, B. Wang, Q. Yuan and W. Zhang, Nickel-Catalyzed Remote C(sp<sup>3</sup>)-N/O Bond Formation of Alkenes with Unactivated Amines and Alcohols, *ACS Catal.*, 2023, **13**, 4409–4420; (e) F. Wu, J. Chang and D. Bai, Synthesis of Sterically Hindered Dialkyl Ethers via Palladium-Catalyzed Fluoro-alkoxylation of gem-Difluoroalkenes, *Org. Lett.*, 2024, **26**, 4953–4957; (f) A. Mifleur, D. S. Mérél, A. Mortreux, I. Suisse, F. Capet, X. Trivelli, M. Sauthier and S. A. Macgregor, Deciphering the Mechanism of the Nickel-Catalyzed Hydroalkoxylation Reaction: A Combined Experimental and Computational Study, *ACS Catal.*, 2017, **7**, 6915–6923; (g) Q. Li, Z. Wang, V. M. Dong and X. Yang, Enantioselective Hydroalkoxylation of 1,3-Dienes via Ni-Catalysis, *J. Am. Chem. Soc.*, 2023, **145**, 3909–3914; (h) S. Yang, A. Han, Y. Liu, X. Tang, G. Lin and Z. He, Catalytic Asymmetric Hydroalkoxylation and Formal Hydration and Hydroaminoxylation of Conjugated Dienes, *J. Am. Chem. Soc.*, 2023, **145**, 3915–3925.

6 (a) L. Ronchin, A. Vavasori and L. Toniolo, Acid catalyzed alkylation of phenols with cyclohexene: Comparison between homogeneous and heterogeneous catalysis, influence of cyclohexyl phenyl ether equilibrium and of the substituent on reaction rate and selectivity, *J. Mol. Catal. A:Chem.*, 2012, **355**, 134–141; (b) C. S. Sevov and J. F. Hartwig, Iridium-Catalyzed, Intermolecular Hydroetherification of Unactivated Aliphatic Alkenes with Phenols, *J. Am. Chem. Soc.*, 2013, **135**, 9303–9306; (c) A. Vasilopoulos, D. L. Golden, J. A. Buss and S. S. Stahl, Copper-Catalyzed C–H Fluorination/Functionalization Sequence Enabling Benzylidic C–H Cross Coupling with Diverse Nucleophiles, *Org. Lett.*, 2020, **22**, 5753–5757; (d) J. M. Balquist and E. R. Degginger, Cyclalkylation of phenol with 1,5-hexadiene, *J. Org. Chem.*, 1971, **36**, 3345–3349; (e) F. J. Sowa, H. D. Hinton, J. A. Nieuwland and J. A. Organic, Reactions with Boron Fluoride. III. The Condensation of Propylene with Phenol, *J. Am. Chem. Soc.*, 1932, **54**, 3694–3698.

7 (a) K. Wu, H. Li, A. Zhou, W. Yang and Q. Yin, Palladium-Catalyzed Chemo- and Regioselective C–H Bond Functionalization of Phenols with 1,3-Dienes, *J. Org. Chem.*, 2023, **88**, 2599–2604; (b) J. Long, C. Dinga and G. Yin, Nickel/Brønsted acid dual-catalyzed regioselective C–H bond allylation of phenols with 1,3-dienes, *Org. Chem. Front.*, 2022, **9**, 3834–3839; (c) Z. Liu, G. Li, T. Yao, J. Zhang and L. Liu, Triflic Acid-Catalyzed Chemo- and Site-Selective C–H Bond Functionalization of Phenols With 1,3-Dienes, *Adv. Synth. Catal.*, 2021, **363**, 2740–2745; (d) G. Wang, L. Gao, H. Chen, X. Liu, J. Cao, S. Chen, X. Cheng and S. Li, Chemoselective Borane-Catalyzed Hydroarylation of 1,3-Dienes with Phenols, *Angew. Chem., Int. Ed.*, 2019, **58**, 1694–1699.

8 N. J. Adamson and S. J. Malcolmson, Catalytic Enantio- and Regioselective Addition of Nucleophiles in the Intermolecular Hydrofunctionalization of 1,3-Dienes, *ACS Catal.*, 2020, **10**, 1060–1076.

9 (a) S. W. M. Crossley, C. Obradors, R. M. Martinez and R. A. Shenvi, Mn-, Fe-, and Co-Catalyzed Radical Hydrofunctionalizations of Olefins, *Chem. Rev.*, 2016, **116**, 8912–9000; (b) G. Zhang and Q. Zhang, Cobalt-catalyzed HAT reaction for asymmetric hydrofunctionalization of alkenes and nucleophiles, *Chem catal.*, 2023, **3**, 100526; (c) Y. Yamaguchi, Y. Seino, A. Suzuki, Y. Kamei, T. Yoshino, M. Kojima and S. Matsunaga, Intramolecular Hydrogen Atom Transfer Hydroarylation of Alkenes toward  $\delta$ -Lactams Using Cobalt-Photoredox Dual Catalysis, *Org. Lett.*, 2022, **24**, 2441–2445; (d) J. Liu, J. Rong, D. P. Wood, Y. Wang, S. H. Liang and S. Lin, Co-Catalyzed Hydrofluorination of Alkenes: Photocatalytic Method Development and Electroanalytical Mechanistic Investigation, *J. Am. Chem. Soc.*, 2024, **146**, 4380–4392; (e) X. Zhou, F. Yang, H. Sun, Y. Yin, W. Ye and R. Zhu, Cobalt-Catalyzed Intermolecular Hydrofunctionalization of Alkenes: Evidence for a Bimetallic Pathway, *J. Am. Chem. Soc.*, 2019, **141**, 7250–7255; (f) S. Jana, V. J. Mayerhofer and C. J. Teskey, Photo- and Electrochemical Cobalt Catalysed Hydrogen Atom Transfer for the Hydrofunctionalisation of Alkenes, *Angew. Chem., Int. Ed.*, 2023, **62**, e202304882.

10 (a) H. Shigehisa, T. Aoki, S. Yamaguchi, N. Shimizu and K. Hiroya, Hydroalkoxylation of Unactivated Olefins with Carbon Radicals and Carbocation Species as Key Intermediates, *J. Am. Chem. Soc.*, 2013, **135**, 10306–10309; (b) H. Shigehisa, M. Hayashi, H. Ohkawa, T. Suzuki, H. Okayasu, M. Mukai, A. Yamazaki, R. Kawai, H. Kikuchi, Y. Satoh, A. Fukuyama and K. Hiroya, Catalytic Synthesis of Saturated Oxygen Heterocycles by Hydrofunctionalization of Unactivated Olefins: Unprotected and Protected Strategies, *J. Am. Chem. Soc.*, 2016, **138**, 10597–10604; (c) K. Ebisawa, K. Izumi, Y. Ooka, H. Kato, S. Kanazawa, S. Komatsu, E. Nishi and

H. Shigehisa, Catalyst- and Silane-Controlled Enantioselective Hydrofunctionalization of Alkenes by Cobalt-Catalyzed Hydrogen Atom Transfer and Radical-Polar Crossover, *J. Am. Chem. Soc.*, 2020, **142**, 13481–13490; (d) T. Nagai, N. Mimata, Y. Terada, C. Sebe and H. Shigehisa, Catalytic Dealkylative Synthesis of Cyclic Carbamates and Ureas *via* Hydrogen Atom Transfer and Radical-Polar Crossover, *Org. Lett.*, 2020, **22**, 5522–5527; (e) A. Osato, T. Fujihara and H. Shigehisa, Constructing Four-Membered Heterocycles by Cycloisomerization, *ACS Catal.*, 2023, **13**, 4101–4110; (f) E. E. Touney, N. J. Foy and S. V. Pronin, Catalytic Radical–Polar Crossover Reactions of Allylic Alcohols, *J. Am. Chem. Soc.*, 2018, **140**, 16982–16987; (g) C. A. Discolo, E. E. Touney and S. V. Pronin, Catalytic Asymmetric Radical–Polar Crossover Hydroalkoxylation, *J. Am. Chem. Soc.*, 2019, **141**, 17527–17532.

11 F. Yang, Y. Nie, H. Liu, L. Zhang, F. Mo and R. Zhu, Electrocatalytic Oxidative Hydrofunctionalization Reactions of Alkenes *via* Co(II/III/IV) Cycle, *ACS Catal.*, 2022, **12**, 2132–2137.

12 S. H Park, J. Jang, K. Shin and H. Kim, Electrocatalytic Radical–Polar Crossover Hydroetherification of Alkenes with Phenols, *ACS Catal.*, 2022, **12**, 10572–10580.

13 M. Nakagawa, Y. Matsuki, K. Nagao and H. Ohmiya, A Triple Photoredox/Cobalt/Brønsted Acid Catalysis Enabling Markovnikov Hydroalkoxylation of Unactivated Alkenes, *J. Am. Chem. Soc.*, 2022, **144**, 7953–7959.

14 M. Guan, L. Zhu, Y. Wang, G. Zhang, H. Miao, B. Chen and Q. Zhang, Cobalt-catalyzed enantioselective hydroetherification of alkenes and symmetric 1,3-diketones, *Chem Catal.*, 2024, **4**, 101126.

15 (a) M. Shen, X. Qi, D. Li, X. Wang, C. Zhu and H. Xu, Cobalt-catalyzed regioselective hydroazidation of 1-aryl-1,3-dienes: facile access to allylic azides, *Org. Chem. Front.*, 2023, **10**, 3010–3015; (b) K. Zhuang, G. C. Haug, Y. Wang, S. Yin, H. Sun, S. Huang, R. Trevino, K. Shen, Y. Sun, C. Huang, B. Qin, Y. Liu, M. Cheng, O. V. Larionov and S. Jin, Cobalt-Catalyzed Carbon–Heteroatom Transfer Enables Regioselective Tricomponent 1,4-Carboamination, *J. Am. Chem. Soc.*, 2024, **146**, 8508–8519.

16 (a) T. Qin, G. Lv, Q. Meng, G. Zhang, T. Xiong and Q. Zhang, Cobalt-Catalyzed Radical Hydroamination of Alkenes with N-Fluorobenzenesulfonimides, *Angew. Chem., Int. Ed.*, 2021, **60**, 25949–25957; (b) H. Miao, M. Guan, T. Xiong, G. Zhang and Q. Zhang, Cobalt-Catalyzed Enantioselective Hydroamination of Arylalkenes with Secondary Amines, *Angew. Chem., Int. Ed.*, 2023, **62**, e202213913; (c) M. Guan, T. Yin, Y. Wang, H. Miao, G. Zhang and Q. Zhang, Cobalt Hydride-Catalyzed Hydroalkynylation of Alkenes with Alkynyl Trifluoroborates, *ACS Catal.*, 2024, **14**, 9294–9301.

17 (a) G. Desimoni, G. Faita and P. Quadrelli, Forty Years after “Heterodiene Syntheses with  $\alpha,\beta$ -Unsaturated Carbonyl Compounds”: Enantioselective Syntheses of 3,4-Dihydropyran Derivatives, *Chem. Rev.*, 2018, **118**, 2080–2248; (b) S. Li, F. Li, J. Gong and Z. Yang, Palladium-Catalyzed Carbonylative Cyclization of Aryl Alkenes/Alkenols: A New Reaction Mode for the Synthesis of Electron-Rich Chromanes, *Org. Lett.*, 2015, **17**, 1240–1243; (c) Y. Yamaguchi, Y. Seino, A. Suzuki, Y. Kamei, T. Yoshino, M. Kojima and S. Matsunaga, Intramolecular Hydrogen Atom Transfer Hydroarylation of Alkenes toward  $\delta$ -Lactams Using Cobalt-Photoredox Dual Catalysis, *Org. Lett.*, 2022, **24**, 2441.

18 D. DiRocco *Electrochemical Series of Photocatalysts and Common Organic Compounds*, Merck, 2014.

19 C. V. Wilson, D. Kim, A. Sharma, R. X. Hooper, R. Poli, B. M. Hoffman and P. L. Holland, Cobalt–Carbon Bonding in a Salen-Supported Cobalt(IV) Alkyl Complex Postulated in Oxidative MHAT Catalysis, *J. Am. Chem. Soc.*, 2022, **144**, 10361–10367.

20 S. Tshepelevitsh, A. Kütt, M. Lõkov, I. Kaljurand, J. Saame, A. Heering, P. G. Plieger, R. Vianello and I. Leito, On the Basicity of Organic Bases in Different Media, *Eur. J. Org. Chem.*, 2019, **2019**, 6735–6748.

21 R. Marcos, C. Rodríguez-Esrich, C. I. Herreras and M. A. Pericàs, Metal-Mediated Cyclization of Aryl and Benzyl Glycidyl Ethers: A Complete Scenario, *J. Am. Chem. Soc.*, 2008, **130**, 16838–16839.

22 N. Elgrishi, D. A. Kurtz and J. L. Dempsey, Reaction Parameters Influencing Cobalt Hydride Formation Kinetics: Implications for Benchmarking H<sub>2</sub>-Evolution Catalysts, *J. Am. Chem. Soc.*, 2017, **139**, 239–244.

23 V. Artero, M. Chavarot-Kerlidou and M. Fontecave, Splitting Water with Cobalt, *Angew. Chem., Int. Ed.*, 2011, **50**, 7238–7266.

24 S. Shibutani, K. Nagao and H. Ohmiya, A Dual Cobalt and Photoredox Catalysis for Hydrohalogenation of Alkenes, *J. Am. Chem. Soc.*, 2024, **146**, 4375–4379.

25 H. Lindner, W. M. Amberg, T. Martini, D. M. Fischer, E. Moore and E. M. Carreira, Photo- and Cobalt-Catalyzed Synthesis of Heterocycles *via* Cycloisomerization of Unactivated Olefins, *Angew. Chem., Int. Ed.*, 2024, **63**, e202319515.

26 H. Yan, Q. Liao, Y. Chen, G. G. Gurzadyan, B. Lu, C. Wu and L. Shi, Photocatalytic Metal Hydride Hydrogen Atom Transfer Mediated Allene Functionalization by Cobalt and Titanium Dual Catalysis, *Angew. Chem., Int. Ed.*, 2023, **62**, e202302483.

27 J. Qin, M. Barday, S. Jana, N. Sanosa, I. Funes-Ardoiz and C. J. Teskey, Photoinduced Cobalt Catalysis for the Reductive Coupling of Pyridines and Dienes Enabled by Paired Single-Electron Transfer, *Angew. Chem., Int. Ed.*, 2023, **62**, e202310639.

28 C.-Y. Tan and S. Hong, Harnessing the potential of acyl triazoles in bifunctional cobalt-catalyzed radical cross-coupling reactions, *Nat. Commun.*, 2024, **15**, 6965.

29 S. L. Shevick, C. Obradors and R. A. Shenvi, Mechanistic Interrogation of Co/Ni-Dual Catalyzed Hydroarylation, *J. Am. Chem. Soc.*, 2018, **140**, 12056–12068.

30 S. Li, F. Li, J. Gong and Z. Yang, Palladium-Catalyzed Carbonylative Cyclization of Aryl Alkenes/Alkenols: A New Reaction Mode for the Synthesis of Electron-Rich Chromanes, *Org. Lett.*, 2015, **17**, 1240–1243.



31 S. N. Anderson, D. H. Ballard, J. Z. Chrzastowski, D. Dodd and M. D. Johnson, A two-stage synthesis of (+)-cis-homocaronic acid from (+)-car-3-ene, *J. Chem. Soc. Chem. Commun.*, 1972, 685–686.

32 R. H. Magnuson, J. Halpern, I. Y. Levitin and M. E. Vol'pin, Stereochemistry of the nucleophilic cleavage of cobalt–carbon bonds in organocobalt(IV) compounds, *J. Chem. Soc. Chem. Commun.*, 1978, 44–46.

33 J. Halpern, J. Topich and K. I. Zamaraev, Electron paramagnetic resonance spectra and electronic structures of organobis(dimethylglyoximato)cobalt(IV) complexes, *Inorg. Chim. Acta*, 1976, **20**, L21–L24.

34 M. E. Vol'pin, I. Y. Levitin, A. L. Sigan, J. Halpern and G. M. Tom, Reactivity of organocobalt(IV) chelate complexes toward nucleophiles: diversity of mechanisms, *Inorg. Chim. Acta*, 1980, **41**, 271–277.

35 S. H. Park, G. Bae, A. Choi, S. Shin, K. Shin, C. H. Choi and H. Kim, Electrocatalytic Access to Azetidines *via* Intramolecular Allylic Hydroamination: Scrutinizing Key Oxidation Steps through Electrochemical Kinetic Analysis, *J. Am. Chem. Soc.*, 2023, **145**, 15360–15369.

